

Synthesis of Core/Shell Colloidal Magnetic Zeolite Microspheres for the Immobilization of Trypsin

By Yonghui Deng, Chunhui Deng, Dawei Qi, Chong Liu, Jia Liu, Xiangmin Zhang, and Dongyuan Zhao*

Colloidal particles with controlled structures, morphologies, and functionalities have attracted much attention because of their potential application in column-packing substrates, photonic crystals, drug delivery, chemical sensors, catalysis carriers, and separation of biomacromolecules.^[1] In particular, colloidal magnetic microspheres have long been of great interest as hybrid materials, because of their perfect combination of easily functionalizable surfaces and magnetic responsiveness. This combination endows them with great potential for use in miniature devices, where easy manipulation, separation, and site-specific targeting via a magnetic field are desired. A variety of approaches have been explored to synthesize magnetic microspheres, including encapsulation of magnetite particles by organic polymers, such as polystyrene,^[2] and coating magnetic particles with inorganic silica via sol-gel processes.^[3] Possible applications of magnetic microspheres have also been explored in fields such as cell sorting, separation of biomolecules, and so on.^[4]

Recently, great efforts have been focused on enhancing the performance of magnetic microspheres. These include efforts to improve their magnetic-field responsiveness, so as to achieve effective manipulation, and efforts to introduce additional functionalities, in order to tailor their physicochemical properties (e.g., high surface area and functional groups) to achieve affinity binding or specific conjugation.^[5] In this regard, we have synthesized submicrometer-sized magnetic microspheres by coating magnetite particles with silica through a modified sol-gel approach; these microspheres proved to be useful in the enrichment of low-abundance peptides.^[6] Based on the hetero-interparticle coalescence strategy, Park et al.^[7] prepared magnetic iron-oxide/Au microspheres, and used them in bioassays. Kim et al.^[8] reported on the production of magnetic fluorescent porous microspheres by simultaneously encapsulating magnetite nanoparticles and CdSe/ZnS quantum dots with mesoporous silica. Shi and coworkers^[9] synthesized magnetic microspheres with disordered mesoporous silica shells. More recently, using a sol-gel synthesis that involved a surfactant, high-magnetization, magnetic, mesoporous, silica microspheres with perpendicularly aligned mesoporous silica shells were reported.^[10] These micro-

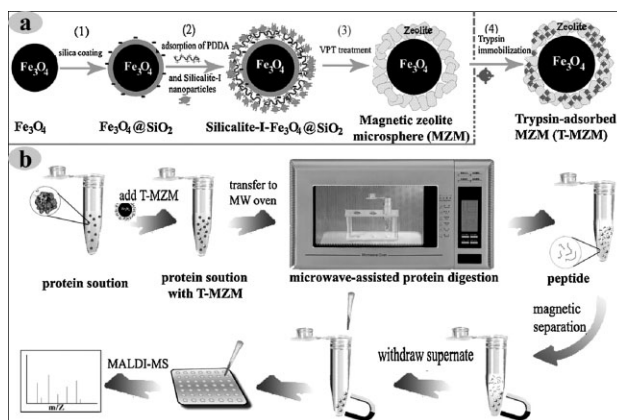
spheres have been used for the efficient removal of microcystins in water. Microporous zeolites are important inorganic materials with open-framework aluminosilicate structures,^[11] and have been extensively used in industrial processes such as gas separation and petrochemical-based catalysis.^[12] Zeolite particles, because of their low-toxicity, good capability, functional groups for grafting or attachment, and high dispersability, have been demonstrated to be good biomaterials in various applications, such as in the immobilization of trypsin for microreactors in microfluidic systems and for the highly efficient enrichment of low-abundance peptides in protein identification.^[13] However, unlike ordered mesoporous silicates (whose synthesis involves self-assembly of a surfactant-templating sol-gel process at low temperatures, e.g., room temperature), zeolites are usually synthesized using high-temperature hydrothermal processes. As a result, the synthesis of core/shell zeolite microspheres remains a great challenge, because of the difficulty in controlling the growth of zeolite crystals on the magnetite particles.

In this communication, we report a novel approach to synthesizing core/shell-structured magnetic zeolite microspheres (MZMs) with uniform variable diameters (from ca. 600 nm to 1 μm). The approach combines sol-gel synthesis of a zeolite seed coating and vapor-phase transport (VPT) for growing the zeolite crystal shells. The colloidal MZMs, which consist of a magnetite core (ca. 400 nm in diameter) and a zeolite shell (ca. 180 nm thick), have a well-defined core/shell structure and a high magnetization of 48.5 emu g^{-1} (emu: electromagnetic units), and exhibit good dispersability in water. Moreover, these microspheres show a strong affinity to trypsin with a high adsorption capacity (62 $\mu\text{g mg}^{-1}$). Using trypsin-immobilized MZMs (T-MZMs), highly efficient protein digestion is achieved, with the assistance of microwave irradiation, in only 15 s, which is much faster than digestion in solution. Moreover, the T-MZMs can be conveniently recovered by simple magnetic separation, and reused at least seven times without any visible reduction in digestion efficiency.

The synthesis procedure for the core/shell MZMs consists of three main steps, as shown in Scheme 1. First, $\text{Fe}_3\text{O}_4/\text{SiO}_2$ microspheres are synthesized by coating Fe_3O_4 particles with a layer of silica via a sol-gel process.^[6,9] The silica layer prevents erosion during the hydrothermal process, and functions as the silica source for the growth of the zeolite crystals. Second, in order to deposit the negatively charged zeolitic seeds on the silica surfaces of the microspheres, a cationic polyelectrolyte, poly(diallyldimethylammonium chloride) (PDDA), was used to modify the surfaces of the $\text{Fe}_3\text{O}_4/\text{SiO}_2$ microspheres; the zeolite seed nanoparticles (silicalite-1) were then adsorbed on the surfaces by Coulomb interaction. Third, the microspheres were subject to

[*] Prof. D. Y. Zhao, Dr. Y. H. Deng, Dr. C. H. Deng, D. W. Qi, C. Liu J. Liu, Prof. X. M. Zhang
Department of Chemistry
Shanghai Key Laboratory of Molecular Catalysis and Innovative Materials
and Advanced Materials Laboratory
Fudan University, Shanghai 200433 (PR China)
E-mail: dyzhao@fudan.edu.cn

DOI: 10.1002/adma.200801766



Scheme 1. a) The synthesis route of and b) the protein-digestion procedure used with the core/shell MZMs. MW: microwave.

VPT treatment by heating at 140 °C in amine vapor to convert the silica to zeolite crystals, and core/shell MZMs were obtained. The Fe_3O_4 particles were synthesized using a modified solvothermal reaction at 200 °C, as reported in the literature.^[6,9] Loose Fe_3O_4 particles with an average diameter of approximately 400 nm were obtained, as revealed by transmission electron microscopy (TEM) images (Fig. 1a). Scanning electron microscopy (SEM) images show that the particles were composed of small magnetite particles about 15 nm in diameter (see Supporting Information, Fig. S1), similar to the results reported previously by Ge et al.^[14] During the sol-gel coating process in a basic water/ethanol solution, silica species from the hydrolysis and condensation of tetraethyl orthosilicate (TEOS) deposited on the Fe_3O_4 particles, resulting in core/shell $\text{Fe}_3\text{O}_4/\text{SiO}_2$ microspheres with silica shells approximately 70 nm thick (Fig. 1b). Nearly spherical silicalite-1 nanoparticles with diameters of ca. 40 nm (Fig. S2) were prepared according to a previously reported method.^[15] The PDPA polyelectrolyte serves as an intermediate for the adsorption of silicalite-1 seed nanoparticles onto the $\text{Fe}_3\text{O}_4/\text{SiO}_2$ microspheres, because both the nanoparticles and microspheres are negatively charged in neutral solution. After the layer-by-layer electrostatic adsorption, the microspheres were homogeneously decorated by silicalite-1 nanoparticles (Fig. 1c and d). The subsequent VPT treatment transformed all the silica to silicalite-1 crystals, resulting in uniform MZMs with Fe_3O_4 particle cores and rough shells (ca. 180 nm thick) composed of large quadrate-shaped zeolite particles (Fig. 1e and f). A high-resolution TEM (HRTEM) image shows ordered lines in the shells of the MZMs, suggesting that the zeolitic shells had good crystalline structures (Fig. 2). Selected-area electron diffraction (SAED) patterns obtained from the edges of the shells of the MZMs are characterized by spotty diffraction rings (Fig. 2, inset), indicating the polycrystallinity of the silicalite-1 structure. As opposed to the parent $\text{Fe}_3\text{O}_4/\text{SiO}_2$ microspheres, the MZMs obtained after VPT treatment exhibited rough surfaces, because of the random growth of the silicalite-1 crystal particles (Fig. 3); these rough surfaces may provide large external surface areas for the adsorption of guest species. Both the TEM and SEM images show that the zeolite crystals on the shells have a quadrate morphology of size 80 nm × 180 nm. It is worth noting that, after calcination and ultrasonication (40 kHz, 120 W) in aqueous solution for 30 min to remove the zeolite template, the

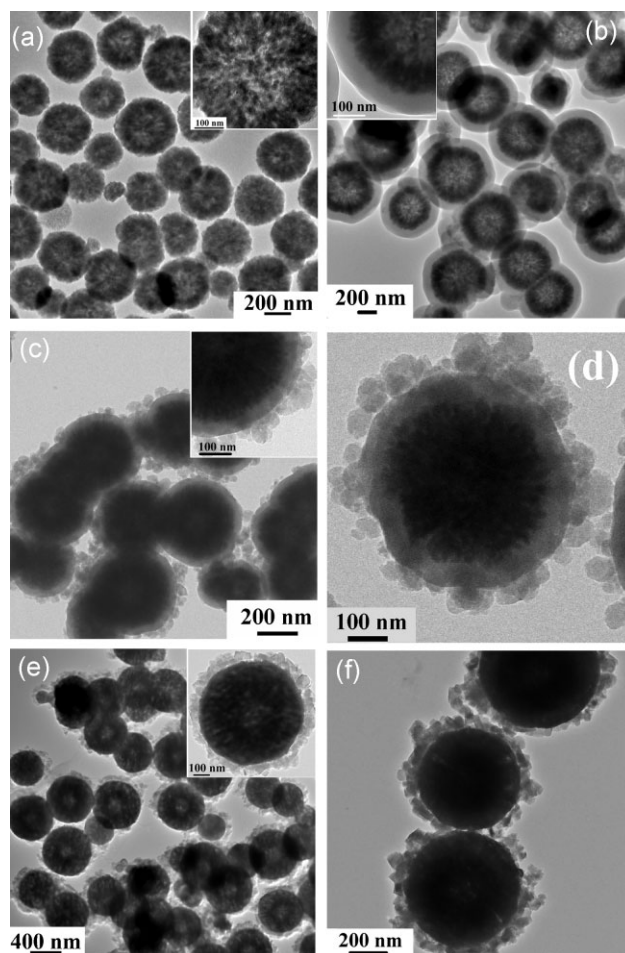


Figure 1. TEM images of a) Fe_3O_4 particles, b) $\text{Fe}_3\text{O}_4/\text{SiO}_2$ microspheres, prepared by coating the magnetite particles with silica via a solution sol-gel process, c,d) $\text{Fe}_3\text{O}_4/\text{SiO}_2$ particles decorated with zeolite, which were obtained after sequential adsorption of PDPA and silicalite-1 nanoseeds, and e,f) MZMs obtained after further VPT treatment of the decorated $\text{Fe}_3\text{O}_4/\text{SiO}_2$ particles at 140 °C for three days.

zeolitic shells of the core/shell MZMs were retained, reflecting the good mechanical and thermal stability of the core/shell microspheres. By using magnetite particles of different diameters, the sizes of the magnetic cores in the MZMs could be adjusted in the range 200–800 nm. Similarly, the thickness of the shells of the MZMs was tunable from 50 to 300 nm, by coating the magnetite particles with silica layers of different thicknesses (20–300 nm) before converting the adsorbed silica-1 nanoseeds.

The VPT method was first developed for converting dry gels to zeolite crystals in the presence of volatile amines, which functioned as structure-directing agents.^[16] In this study, the layered amorphous SiO_2 in the $\text{Fe}_3\text{O}_4/\text{SiO}_2$ microspheres served as a “nutrition pool” during the VPT process, and the zeolite nanoparticles adsorbed on the microspheres acted as seeds for in situ growth, by consuming the amorphous silica in the presence of the amine vapors. The MZMs obtained after VPT treatment displayed typical X-ray diffraction peaks with higher intensities and narrower peak widths (Fig. S3 in the Supporting Information) than those of $\text{Fe}_3\text{O}_4/\text{SiO}_2$ microspheres decorated

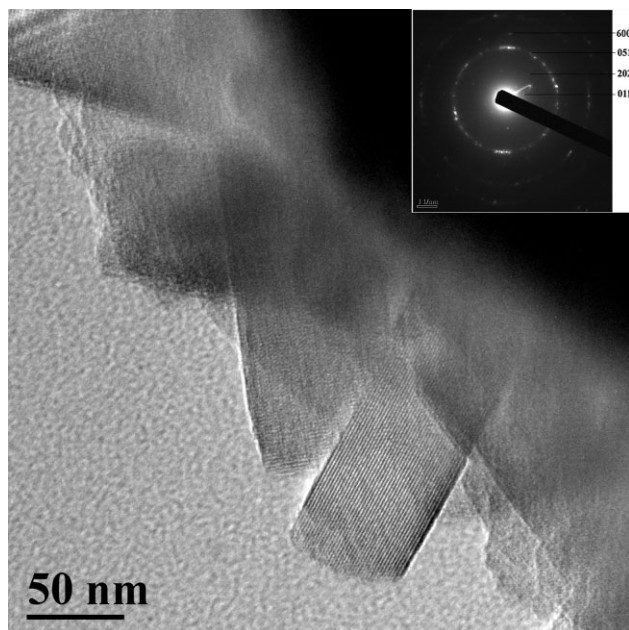


Figure 2. HRTEM image of the core/shell magnetic zeolite microspheres and selected-area electron diffraction pattern recorded from the edge of the MZMs (inset).

with zeolite nanoparticles; this can be assigned to the MFI zeolite structure (silicate-1 structure, International Zeolite Association). This result indicates a significant increase in the weight fraction of silicalite-1 in the MZM products, as a result of the depletion of silica and the growth of the zeolite crystals.

The magnetization saturation values of the magnetite particles and the core/shell MZMs were measured at 300 K to be 82.0 and 48.5 emu g^{-1} , respectively, suggesting a high magnetite content (about 59 wt%) in the MZMs. As can clearly be seen from the magnetic hysteresis loops (Fig. 4), both the magnetite particles and core/shell MZMs exhibit super-paramagnetism, that is, no magnetization remains when the applied magnetic field is removed. This is because of the small size of the building blocks of the magnetite particles. Thanks to their hydrophilic surfaces, it was possible to disperse the MZMs (0.10 g) in water (100 mL) by ultrasonication. No visible sedimentation occurred after standing for at least 6 h, suggesting good dispersibility of the MZMs. Because of their high magnetite contents, the MZMs were easily separated from the dispersion in 60 s using a magnet (1000 Oe;

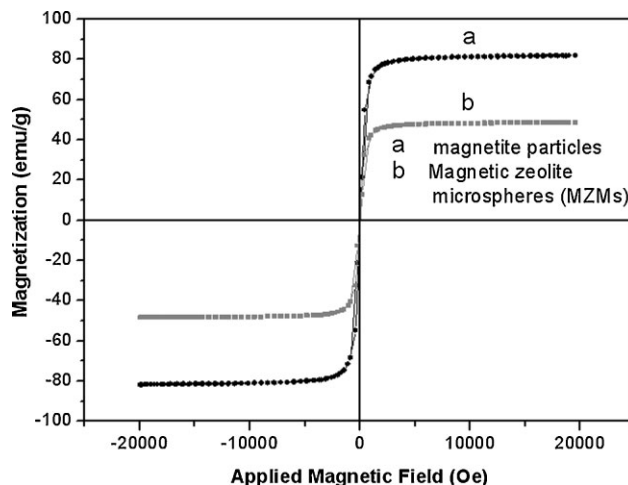


Figure 4. Hysteresis loops recorded at 25 °C of a) the magnetite particles and b) the MZMs.

1 Oe = 1000/4 π A m $^{-1}$). Their super-paramagnetic properties enabled their redispersion by light sonication once the magnetic field was removed (Fig. S4 in the Supporting Information). These properties are very important in achieving fast particle manipulation in applications.

Colloidal zeolite particles have been shown to be efficient substrates for immobilizing trypsin for use in protein digestion, because of their large external surface areas and affinity for trypsin molecules.^[13] The core/shell MZMs possess zeolite surfaces and a unique magnetic responsivity, which render them promising candidates for use as magnetically separable substrates for the immobilization of trypsin, which is then used in protein digestion. A protocol was designed to explore the possibility of using the MZMs produced here for the immobilization of trypsin, and its subsequent use in protein digestion (Scheme 1b). Firstly, the trypsin was immobilized onto the microspheres in a NH_4HCO_3 buffer. The UV absorption spectrum shows that as much as 62 $\mu\text{g mg}^{-1}$ of trypsin was immobilized on the MZMs. This large amount is mainly due to the strong Coulomb forces that exist between the negatively charged zeolitic surfaces of the Fe_3O_4 /Zeolite microspheres and the positively charged trypsin molecules in the NH_4HCO_3 buffer. Second, the T-MZMs were mixed with a protein solution in preparation for microwave-assisted protein digestion.^[17] Finally, after convenient removal of the T-MZMs by magnetic separation, the digested proteins were subjected to peptide mapping, wherein the individual peptide fragments were detected of by matrix-assisted laser desorption/ionization time-of-flight mass spectrometry (MALDI-TOF MS).

In order to demonstrate the digestion efficiency, three standard proteins with multiple cleavage sites, cytochrome c (cyt-c, MW:12 384), myoglobin (MYG, MW: 17 000), and bovine serum albumin (BSA, MW: 66 000) were used as model substrates. After digestion, the immobilized trypsin was easily isolated from solution using a magnet. The peptide analysis of cyt-c, MYG, and BSA on the T-MZMs after the

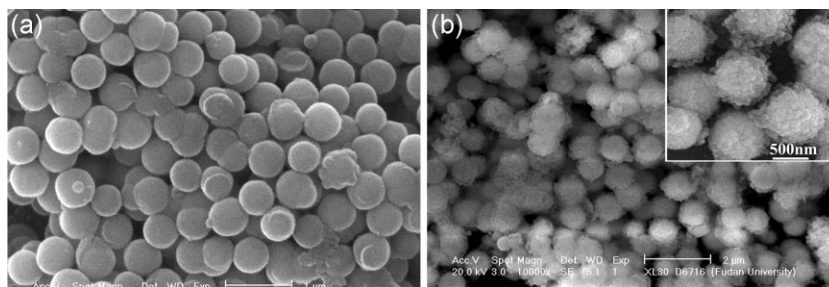


Figure 3. SEM images of core/shell a) $\text{Fe}_3\text{O}_4/\text{SiO}_2$ microspheres and b) MZMs. The inset in b) shows the MZMs at high magnification.

microwave-assisted protein digestion for the short period of 15 s indicated the presence of many digestion fragments (Fig. 5). The sequence coverages obtained from the database are 77% for cyt-c, 89% for MYG, and 25% for BSA (Table S1, Supporting Information). For comparison, protein digestion was also performed for 12 h using free trypsin in solution. Mass spectra measurements indicated equivalent or better digestion efficiencies for cyt-c and MYG in the 15 s microwave-assisted digestion using the T-MZMs (Fig. 6 and Table S2, Supporting Information). For

BSA, the number of originated peptides obtained by digestion using the T-MZMs was slightly less than that obtained from the conventional method, but the proteins were still positively identified. Taking the greatly reduced incubation time into account, it can be concluded that the digestion efficiency is significantly improved using T-MZMs as substrates. Such high efficiency can be explained by the large capacity of the MZMs for trypsin immobilization and the presence of Fe₃O₄ particles, which are excellent microwave absorbers.^[18] To test the stability and reusability of the T-MZMs, seven consecutive digestion runs were conducted with MYG. No obvious decrease in the sequence coverage was observed (Fig. S5, Supporting Information), suggesting good retention of the activity of the T-MZMs.

In summary, the synthesis of functional core/shell MZMs consisting of magnetite cores (ca. 400 nm in diameter) and rough zeolite silicalite-1 shells (ca. 180 nm thick) has been demonstrated. The synthesis occurs via a novel approach that combines the sol-gel coating of zeolite seeds with a VPT technique for growing zeolite crystals. Because of the high affinity for trypsin (62 μg mg⁻¹) and excellent microwave-absorption ability of the magnetite cores, highly efficient and rapid protein digestion was realized in only 15 s. The microspheres could be reused at least seven times without any visible reduction in their protein-digestion efficiency. Because of their useful surface properties and magnetic responsiveness, these microspheres may be utilized in other applications, such as cell separation and drug delivery.

Experimental

Materials and Chemicals: Trifluoroacetic acid (TFA) was purchased from Merck (Darmstadt, Germany). BSA (fraction V) was obtained from Bio Basic Inc (Toronto, Canada). Trypsin treated with tosyl-L-phenylalanyl chloromethyl ketone (TPCK), cyt-c (EC 232-700-9), MYG, sinapinic acid, and α-cyano-4-hydroxycinnamic acid (CHCA) were purchased from Sigma Chemical Company (St. Louis, MO). Water was purified using a MilliQ system (Millipore, Molsheim, France). All other chemicals were of analytical grade and used as received.

Synthesis of Core/Shell Magnetic Zeolite Microspheres: In a typical synthesis, 5.0 g of dispersed Fe₃O₄/SiO₂ microspheres (4.0 wt%, see Supporting Information) was mixed with 2.0 g of PDDA (*M_w* = 20 000 g mol⁻¹) in an aqueous solution (1.0 wt%) for PDDA adsorption. The Fe₃O₄/SiO₂ microspheres with adsorbed PDDA were then separated using a magnet, and washed four times in an aqueous NH₄OH solution (2.0 wt%). The Fe₃O₄/SiO₂ microspheres were then redispersed in 10 mL of the silicalite-1 nanoparticle dispersion (1.0 wt%) for adsorption of the seeds. The Fe₃O₄/SiO₂ microspheres decorated with silicalite-1 nanoparticles were separated and washed four times in an aqueous NH₄OH solution (2.0 wt%). The microspheres obtained were loaded in a crucible with a

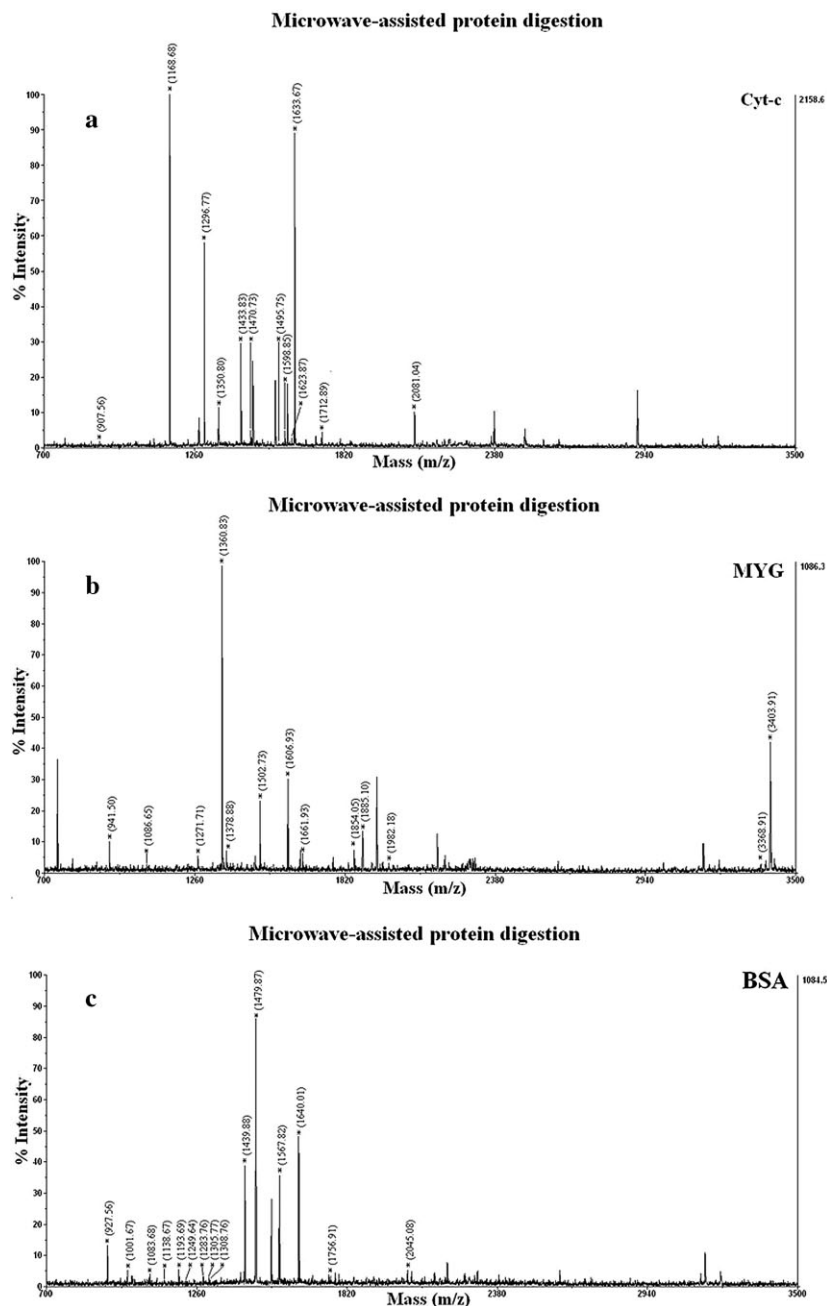


Figure 5. MALDI-TOF MS spectra of tryptic peptides originating from a) Cyt-c, b) MYG, and c) BSA, using T-MZMs as a substrate after microwave-assisted digestion for 15 s. The asterisks indicate the peptides obtained from standard proteins.

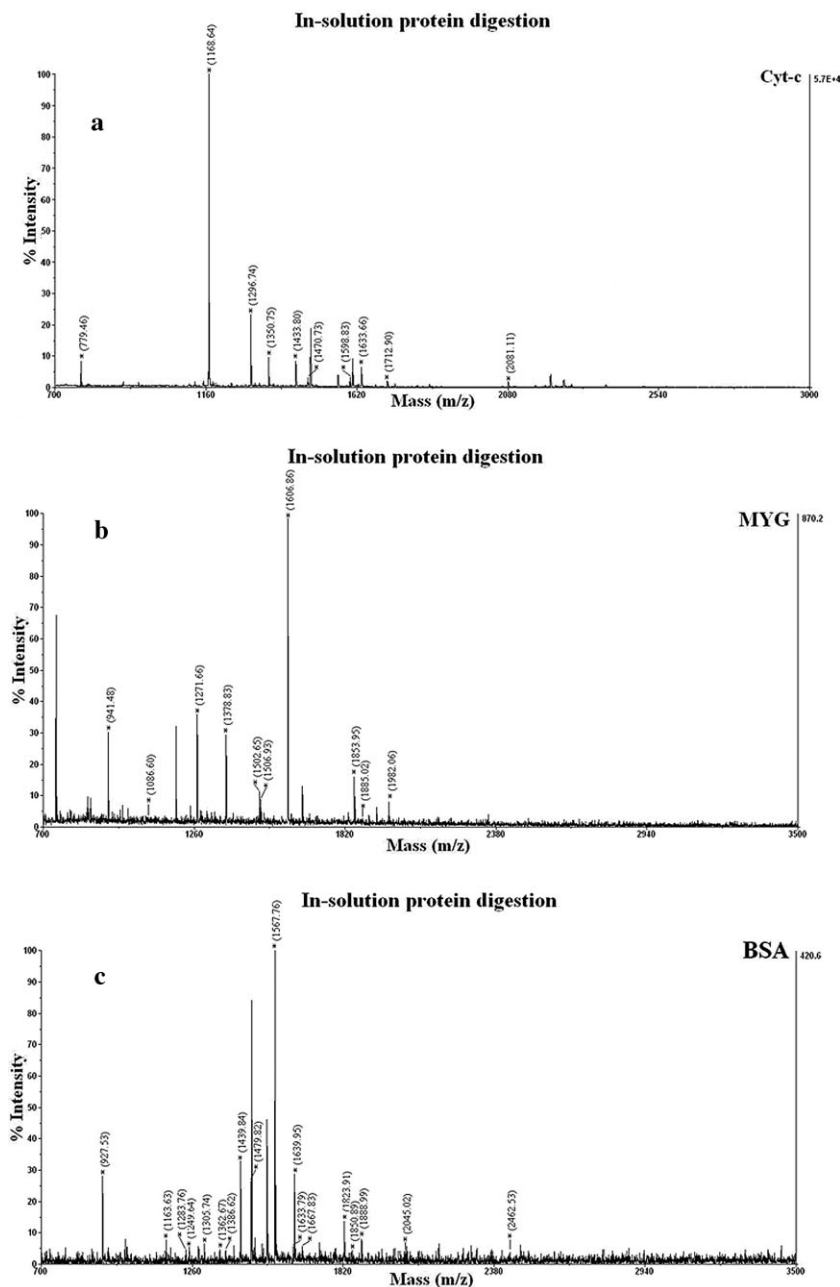


Figure 6. MALDI-TOF MS spectra of tryptic peptides originating from a) Cyt-c, b) MYG, and c) BSA after conventional in-solution digestion for 12 h. The asterisks indicate peptides obtained from standard proteins.

capacity of 5 mL, and vacuum dried at 30 °C. The crucible with the dried microsphere powder was then placed in an autoclave (100 mL in capacity), in which a liquid mixture of triethylamine (2.0 g), ethylenediamine (0.1 g), and water (0.4 g) was added in advance. The autoclave was then enclosed and heated in an oven at 140 °C for three days. After cooling, the product was washed with ethanol and then dried in vacuum.

Protein Digestion

Enzyme Immobilization: MZMs (1.0 mg) were incubated with TPCK-treated trypsin solution (1.5 mL, 1.0 mg mL⁻¹, 25 mM NH₄HCO₃

as buffer) for 1 h under gentle rotation at room temperature. After reacting, the excess trypsin solution was removed with the help of a magnet. The trypsin-immobilized MZMs were washed with NH₄HCO₃ buffer (25 mM, 200 μL) and stored before use. After trypsin immobilization, UV adsorption measurements were conducted on all the supernatants of the reaction, including the TPCK-treated trypsin solution before and after immobilization, and the four buffer solutions used for washing. The amount of immobilized trypsin was calculated by comparing the UV adsorption value of the supernatant before and after immobilization. The UV-absorption values of the supernatant solution were measured at a wavelength of 280 nm.

Microwave-Assisted Protein Digestion: Three standard proteins, cyt-c, MYG, and BSA, were used as model substrates to evaluate digestion performance. Typically, 0.2 mg of the protein was dissolved in a NH₄HCO₃ buffer (25 mM, 1.0 mL). 0.2 mg of T-MCMs was transferred to 40 μL of the protein solution (0.20 μg μL⁻¹) in a 0.6 mL Eppendorf tube. A domestic microwave oven (maximum output power 700 W) was used to conduct the microwave-assisted protein digestion. After microwave irradiation for 15 s, the supernatant was deposited directly onto a MALDI plate using an external magnet to extract the microspheres.

Solution Digestion of Proteins: For comparison, the digestion of cyt-c, MYG, and BSA was also performed according to conventional procedures using trypsin as a catalyst in solution. The standard proteins were first denatured in a 25 mM NH₄HCO₃ buffer containing 8.0 M urea for 1 h at 37 °C, before being diluted with a 25 mM NH₄HCO₃ buffer (pH 7.7) to reduce the concentration of urea to below 1.0 M. The digestion was performed by adding trypsin to the protein solution at a substrate/enzyme ratio of 40:1, and the solution was incubated at 37 °C for 12 h. After digestion, 1.0 μL of formic acid was added to the solution to stop the reaction.

MALDI-TOF-MS: Sample solutions were deposited on the MALDI plate using the dried-droplet method. A total of 0.5 μL of the sample solution was dropped onto the MALDI plate, to which 0.5 μL of the CHCA matrix solution (5.0 mg mL⁻¹, 0.1% TFA in 50% acetonitrile aqueous solution) was introduced. Positive-ion MALDI-TOF mass spectra were acquired using a 4700 Proteomics Analyzer (Applied Biosystem). Sample desorption was achieved using a Nd:YAG laser (355 nm; YAG: yttrium aluminum garnet) operating at a repetition rate of 200 Hz and an acceleration voltage of 20 kV.

Acknowledgements

This work was supported by the NSF of China (20721063, 20521140450, 20871030, 20875017), the State Key Basic Research Program of PRC (2006CB202502), Shanghai Sci. & Tech. Foundation (06DJ14006), Shanghai Leading Academic Discipline Project (B108), the Agilent Technologies Foundation (0214), and the Shanghai Rising-Star Program (08QA14010). Supporting Information is available online from Wiley InterScience or from the author.

Received: June 24, 2008

Revised: September 20, 2008

Published online: January 12, 2009

- [1] a) J. G. Yu, H. T. Guo, S. A. Davis, S. Mann, *Adv. Funct. Mater.* **2006**, *16*, 2035; b) P. M. Arnal, C. Weidenthaler, F. Schuth, *Chem. Mater.* **2006**, *18*, 2733; c) H. Lee, E. Lee, D. K. Kim, N. K. Jang, Y. Y. Jeong, S. Y. Jon, *J. Am. Chem. Soc.* **2006**, *128*, 7383; d) G. Ibarz, L. Dahne, E. Donath, H. Mohwald, *Adv. Mater.* **2001**, *13*, 1324.
- [2] a) X. L. Xu, G. Friedman, K. D. Humfeld, S. A. Majetich, S. A. Asher, *Adv. Mater.* **2001**, *13*, 1681; b) Y. H. Deng, L. Wang, W. L. Yang, S. K. Fu, A. Elaissari, *J. Magn. Magn. Mater.* **2003**, *257*, 69; c) B. D. Korth, P. Keng, I. Shim, S. E. Bowles, C. B. Tang, T. Kowalewski, K. W. Nebesny, J. Pyun, *J. Am. Chem. Soc.* **2006**, *128*, 6562; d) J. P. Ge, Y. X. Hu, T. R. Zhang, Y. D. Yin, *J. Am. Chem. Soc.* **2007**, *129*, 8974.
- [3] a) Y. Lu, Y. D. Yin, Z. Li, Y. Y. Xia, *Nano Lett.* **2002**, *2*, 785; b) Y. H. Deng, C. C. Wang, J. H. Hu, W. L. Yang, S. K. Fu, *Colloids Surf, A.* **2005**, *262*, 87; c) J. Sudimack, R. J. Lee, *Adv. Drug Delivery Rev.* **2000**, *41*, 147.
- [4] a) Y. Weizmann, F. Patolsky, E. Katz, I. Willner, *J. Am. Chem. Soc.* **2003**, *125*, 3452. b) Y. Li, X. Q. Xu, D. W. Qi, C. H. Deng, P. Y. Yang, X. M. Zhang, *J. Proteome Res.* **2008**, *7*, 2526. c) Y. Li, D. W. Qi, C. H. Deng, P. Y. Yang, X. M. Zhang, *J. Proteome Res.* **2008**, *7*, 1767. d) S. Santra, R. P. Bagwe, D. Dutta, J. T. Stanley, G. A. Walter, W. Tan, B. M. Moudgil, R. A. Mericle, *Adv. Mater.* **2005**, *17*, 2165. e) Y. Li, H. Q. Lin, C. H. Deng, P. Y. Yang, X. M. Zhang, *Proteomics* **2008**, *8*, 238.
- [5] a) Y. H. Deng, W. L. Yang, C. C. Wang, S. K. Fu, *Adv. Mater.* **2003**, *15*, 1729; b) Y. H. Deng, C. C. Wang, X. Z. Shen, W. L. Yang, S. K. Fu, *Chem. Eur. J.* **2005**, *11*, 6006; c) T. Sen, A. Sebastianelli, I. J. Bruce, *J. Am. Chem. Soc.* **2006**, *128*, 7130; d) V. Salgueirino-Maceira, M. A. Correa-Duarte, M. Farle, A. Lopez-Quintela, K. Sieradzki, R. Diaz, *Chem. Mater.* **2006**, *18*, 2701.
- [6] X. Xu, C. H. Deng, M. Gao, W. Yu, P. Yang, X. Zhang, *Adv. Mater.* **2006**, *18*, 3289.
- [7] H. Y. Park, M. J. Schadt, L. Y. Wang, I. S. Lim, P. N. Njoki, S. H. Kim, M. Y. Jang, C. J. Zhong, *Langmuir* **2007**, *23*, 9050.
- [8] J. Kim, J. E. Lee, J. Lee, J. H. Yu, B. C. Kim, K. An, Y. Hwang, C. H. Shin, J. G. Park, J. Kim, T. Hyeon, *J. Am. Chem. Soc.* **2006**, *128*, 688.
- [9] W. R. Zhao, J. L. Gu, L. X. Zhang, H. R. Chen, J. L. Shi, *J. Am. Chem. Soc.* **2005**, *127*, 8916.
- [10] Y. H. Deng, D. W. Qi, C. H. Deng, X. M. Zhang, D. Y. Zhao, *J. Am. Chem. Soc.* **2008**, *130*, 28.
- [11] W. M. Meier, D. H. Olson, Ch. Baerlocher, *Atlas of Zeolite Structure Types*, Elsevier, Boston, MA **1996**.
- [12] D. W. Breck, *Zeolite Molecular Sieves*, Wiley, New York 1974.
- [13] a) A. Corma, V. Fornes, F. Rey, *Adv. Mater.* **2002**, *14*, 71; b) Y. H. Zhang, Y. Liu, J. L. Kong, P. Y. Yang, Y. Tang, B. H. Liu, *Small* **2006**, *2*, 1170; c) Y. H. Zhang, X. Y. Wang, W. Shan, B. Y. Wu, H. Z. Fan, X. J. Yu, Y. Tang, P. Y. Yang, *Angew. Chem. Int. Ed.* **2005**, *44*, 615; d) A. Tavoraro, P. Tavoraro, E. Drioli, *Colloids Surf, B* **2007**, *55*, 67.
- [14] J. P. Ge, Y. X. Hu, M. Biasini, W. P. Beyermann, Y. D. Yin, *Angew. Chem. Int. Ed.* **2007**, *46*, 4342.
- [15] K. H. Rhodes, S. A. Davis, F. Caruso, B. J. Zhang, S. Mann, *Chem. Mater.* **2000**, *12*, 2832.
- [16] M. H. Kim, H. X. Li, M. E. Davis, *Microporous Mater.* **1993**, *1*, 191.
- [17] N. B. Pramanik, U. A. Mirza, Y. H. Ning, Y. H. Liu, P. L. Bartner, P. C. Weber, A. K. Bose, *Protein Sci.* **2002**, *11*, 2676.
- [18] a) W. Y. Chen, Y. C. Chen, *Anal. Chem.* **2007**, *79*, 2394; b) S. Lin, D. Yun, D. Qi, C. Deng, Y. Li, X. Zhang, *J. Proteome Res.* **2008**, *7*, 1297.